CHAPTER III
LITERATURE REVIEWS

Chapter III reviews the literatures of the giant dielectric properties of NiO-based ceramics and the explanations for up to date of the origin of the observed giant dielectric response in the NiO-based ceramics. The giant dielectric constant in the NiO-based ceramics can be achieved by co-doping pure-NiO with two types of ions—monovalent cations (i.e., Li^+, Na^+, and K^+) and high-valent cations (e.g., Al^{3+}, Ti^+, Si^{4+}, V^{5+}, Ta^{5+}, and W^{6+}). The former type of the doping is used to transform the insulating property of the bulk NiO ceramic to semiconducting property, and the latter type is used to promote insulating grain boundaries. The insulating grain boundaries are introduced by the accumulation of second phases, forming from the high-valent cations and NiO matrix, along the grain boundaries. The effect of the doping with different types of ions on the microstructure and dielectric properties of the NiO-based ceramics is also explored in this chapter.

3.1 Giant dielectric properties of Li and Ti co-doped NiO ceramics

Nickel oxide (NiO) is an insulating material with complex band structure (Zaanen et al., 1985; Mettheiss, 1972a,b). Pure NiO is classified as a 'Mott–Hubbard insulator' with room temperature conductivity less than 10^{-13} Scm^{-1} (Biju, Khadar, 2001) in which electrical conduction at room temperature is due to holes. However, the low conductivity of NiO can dramatically be increased by introduction of Ni^{2+} vacancies and/or doping with monovalent impurities like Li^+ (Van Elp et al., 1992). Although the electrical properties of NiO have been studied extensively over many years, a clear understanding of the involved mechanisms is still missing.

In general, the dielectric constant of the prefect NiO ceramic is about 30 at room temperature (Lin et al., 2004; 2005b). However, it has been reported that the dielectric constant of the NiO ceramic could be increased up to the range of 10^4–10^5 by co-doping with Li and Ti ions with the chemical formula as $Li_xTi_yNi_{1-x-y}O$ (abbreviated as LTNO) (Wu J et al., 2002). Moreover, this giant dielectric constant

was also found to be nearly temperature independent over temperature range of 200–400 K, as depicted in figure 3.1. This figure demonstrates the temperature dependence of the dielectric constant (ε') and the loss tangent ($\tan\delta$) of the $Li_{0.05}Ti_{0.02}Ni_{0.93}O$ ceramic prepared by a simple sol-gel method at different frequencies. A plateau of the dielectric spectra was observed at frequencies below 10^4 Hz over the measuring temperature range. With increasing the frequency up to 10^5 Hz, however, the rapid decrease in the dielectric constant was observed at a low temperature range, corresponding to the existence of the loss tangent peak. Both of the rapid decrease in the dielectric constant and the related relaxation peak of the loss tangent shifted to a higher temperature range with increasing the frequency. This indicates to the thermally activated mechanism of this dielectric relaxation process. The dielectric relaxation behavior of the LTNO ceramic was ascribed based on the fact that electric dipoles will freeze through the relaxation process at low temperature, and there exists decay in polarization with respect to an applied electric field. As a result, the intensity of polarization decreases. This can cause a change in the dielectric constant—the dramatic drop of the value of the dielectric constant as clearly seen in figure 3.1(a).

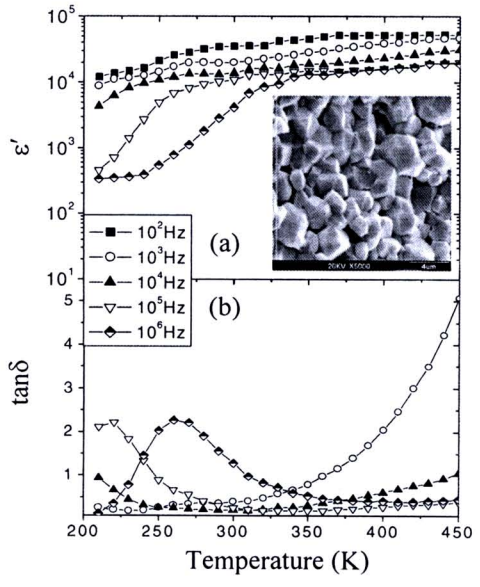

Figure 3.1 Temperature dependence of (a) dielectric constant (ε′) and (b) loss tangent (tanδ) of the $Li_{0.05}Ti_{0.02}Ni_{0.93}O$ ceramic at various frequencies. The inset shows SEM image (Adapted from Wu J et al., 2002).

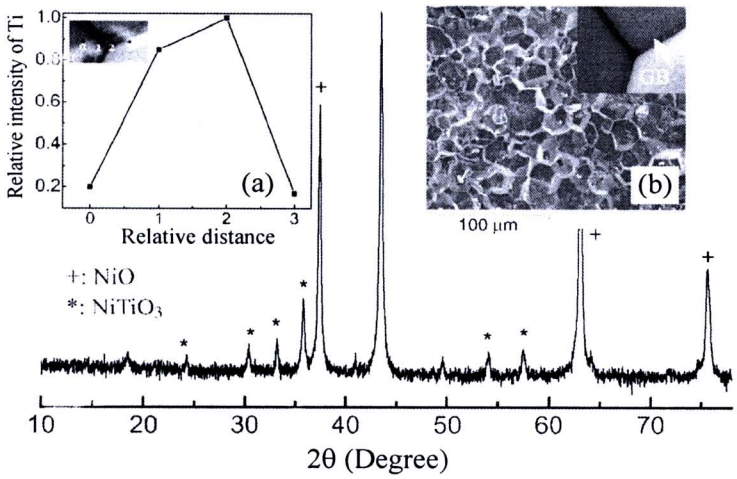

Figure 3.2 XRD pattern of the $Li_{0.10}Ti_{0.05}Ni_{0.85}O$ ceramic; inset (a) is Ti element profile obtained from the EDS spectra; inset (b) is the SEM image of the fractured surface of the $Li_{0.10}Ti_{0.02}Ni_{0.88}O$ ceramic (Adapted from Lin et al., 2006a).

Due to NiO is a non-ferroelectric material, the observed giant dielectric response in the LTNO polycrystalline ceramics might be related to the effect of grain and grain boundary just like $CaCu_3Ti_4O_{12}$ ceramics (Sinclair et al., 2002; Chung et al., 2004). To clarify this assumption, the microstructure and the phase composition of the LTNO ceramics were characterized by x-ray diffraction (XRD) and scanning electron microscopy (SEM), respectively. The XRD and SEM results of LTNO ceramics were revealed in figure 3.2 (Lin et al., 2006a). The XRD pattern of the $Li_{0.10}Ti_{0.05}Ni_{0.85}O$ ceramic revealed the main phase of NiO and the second phase of $NiTiO_3$. The microstructure of the $Li_{0.05}Ti_{0.02}Ni_{0.93}O$ ceramic was revealed in the inset (a), showing an obvious grain and grain boundary structure. The thickness of the grain boundary estimated from the SEM image was found to be about 30 nm. The chemical compositions of the grain and grain boundary were investigated by using an energy dispersive x-ray spectroscopy (EDS) technique. The EDS results indicated that Ti dopant was rich along the grain boundaries, but indigent in the grains. Consequently, based on this research, the shell of the grain was regarded as a Ti-rich boundaries (e.g., $NiTiO_3$), while the core of the grain was Li-doped NiO particles, which is well

known as a semiconductor. The giant dielectric and the related electrical properties of the LTNO ceramics were expected to be associated with this special microstructure.

According to the microstructure and phase composition analyses, the difference in electrical properties between the grain and grain boundary may be produced due to the different chemical compositions between them. The electrical conductivity of the grain and grain boundary of the LTNO ceramics was studied by using an impedance spectroscopy, which is a powerful tool in separating out the bulk and grain boundary effects (Morrison et al., 2001; Sinclair et al., 2002). As shown in figure 3.3 (Lin et al., 2006a), the impedance semicircles of the $Li_{0.10}Ti_{0.05}Ni_{0.85}O$ ceramic become larger with decreasing temperature. When the temperature was sufficiently low, another impedance semicircle was observed, as displayed in the inset. The observation of two semicircles strongly suggested that the LTNO ceramics were electrically heterogeneous, confirming the assumption. This heterogeneous structure consists of semiconducting grains (Li-doped NiO grains) and insulating grain boundaries (Ti-rich boundaries). Therefore, the core/shell structural model could be employed for further analysis. The observed semicircles at high and low temperatures can usually be assigned to the effect of charge transport within the grain and grain boundary, respectively (Sinclair et al., 2002). The charge transport inside the grain should be mainly affected by the addition of Li ions in NiO, leading to an increase in the electrical conductivity of the grains. Generally, for every added Li^+, one Ni^{2+} is promoted to the Ni^{3+} state, which is the lost electron filling a state in the oxygen *2p* valence band. The lattice now contains Ni^{2+} and Ni^{3+} ions on equivalent sites and is the model situation for conduction by polaron hopping (Moulson, Herbert, 2003). According to the polaronic scenario, the temperature dependence of the conductivity (σ) was, with a temperature dependence prefactor, ascribed as (Bosman, van Daal, 1970),

$$\sigma_{polaron} \propto T^{-1} \exp(-E / k_B T), \tag{3.1}$$

where E, k_B, and T are the conduction activation energy, Boltzmann constant, and absolute temperature, respectively. It was suggested that the grain boundary effect on

electric conductivity may originate from a grain boundary potential barrier, which should be ascribed by the Ti-rich boundary for the (Li, Ti)-doped NiO ceramics system (Lin et al., 2006a). As shown in figure 3.3, the conductivity data of the grain (σ_g) and grain boundary (σ_{gb}) at various temperatures were estimated from the diameter of each impedance semicircle. As results, the conduction activation energies inside the grain (E_g) and at the grain boundary (E_{gb}) could be calculated by using equation (3.1), and were found to be 0.377 and 0.439 eV, respectively. These results strongly indicated that the grain and grain boundary of the LTNO ceramics had different electrical transport characters, forming an electrically heterogeneous structure.

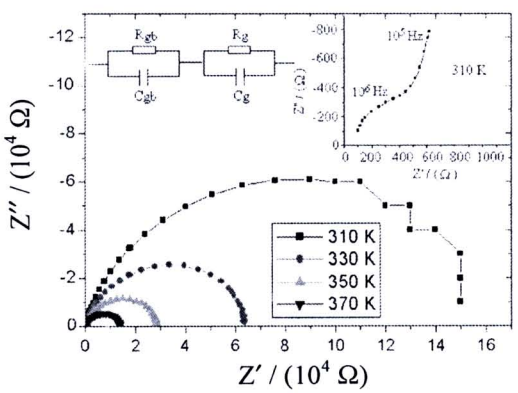

Figure 3.3 Impedance spectra as a function of temperature for the $Li_{0.10}Ti_{0.05}Ni_{0.85}O$ ceramic; inset is the equivalent circuit. The small semicircle arc is displayed in the inset of the impedance spectrum at high frequency and 310 K (Adapted from Lin et al., 2006a).

Based on these analyses, it has been believed that the giant dielectric response in the LTNO ceramics is attributed to an internal barrier layer capacitance (IBLC) effect, which can be ascribed by the Maxwell-Wagner polarization mechanism (Lin et al., 2006a). Under an electric field, the movement of charge carriers inside the semiconducting grains of the LTNO ceramics is restricted by the insulating barriers at the grain boundaries. The accumulation of charges at the grain boundaries produces

the space charge polarization at these regions. This is responsible for the observed giant dielectric response in the LTNO ceramics.

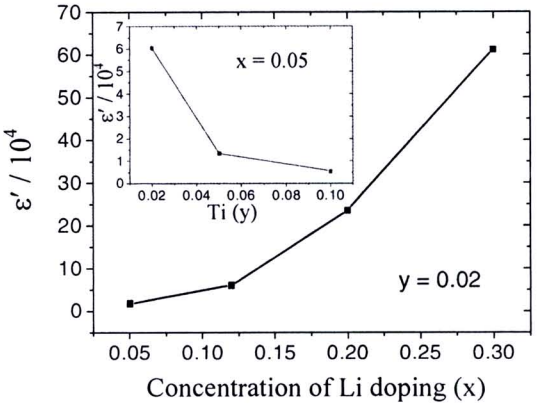

Figure 3.4 The dependence of the dielectric constant (ε′) at room temperature and frequency of 10^3 Hz on the concentration of Li and Ti (see the inset) doped in $Li_xTi_yNi_{1-x-y}O$ ceramics (Adapted from Wu J et al., 2002).

Interestingly, the dielectric constant of the LTNO ceramics could be tuned by varying the concentration of the Li and Ti doping, as shown in figure 3.4 (Wu J et al., 2002). The dielectric constants of the LTNO ceramics could be enhanced or decreased by increasing the Li or Ti doping concentrations, respectively. These interesting experimental results might be attributed to that the amounts of charge carriers inside the LTNO's grains can be increased by increasing the Li doping concentration. Therefore, under an applied electric field, more accumulated charges at the grain boundaries were able to enhance the space charge polarization intensity; consequently, the dielectric constant of the LTNO ceramics with higher Li doping concentration would increase. According to a simple series layer model for IBLC materials (Wu J et al., 2002), $\varepsilon' = \varepsilon_{gb} d / t$, where ε_{gb} is the dielectric constant of the grain boundary, d is the grain size, and t is the boundary-layer thickness, the observed decrease in the dielectric constant was suggested to the increase in the grain boundary thickness. Because most Ti doping ions were detected at the grain

boundaries forming the insulating phase of $NiTiO_3$, as proved in figure 3.2, thus t would be increased with increasing the Ti doping concentration.

Normally, a dielectric relaxation behavior of materials can provide important clues concerning with the related mechanism (Macdonald, 2005). Besides the giant dielectric constant, the dielectric relaxation behavior of the LTNO ceramics could be observed from their dielectric spectra. As demonstrated in figure 3.5, at the temperature of 210 K, the rapid decrease in the dielectric constant and the corresponding relaxation peak of the loss tangent were appeared, suggesting to the relaxation behavior. The thermally activated mechanism was suggested by the movement of the steplike decrease and the relaxation peak, which shifted to higher frequency with increasing the temperature. This dielectric relaxation was empirically ascribed by Debye-like or Cole-Cole relaxation model (Cole, Cole, 1941),

$$\varepsilon^* = \varepsilon' - j\varepsilon'' = \varepsilon'_\infty + \frac{\varepsilon'_s - \varepsilon'_\infty}{1+(j\omega\tau)^\alpha}, \tag{3.2}$$

where ε'_s and ε'_∞ are respectively the static and high frequency limits of dielectric constant, τ is the relaxation time, and α is a constant ($0 < \alpha \leq 1$). For an ideal Debye relaxation, α=1. If α<1, it implies that the relaxation has a distribution of relaxation times (Liu J et al., 2005; Thongbai et al., 2007), leading to a broader peak shape than a Debye peak.

According to the fitted results, the values of τ were obtained at various temperatures. The temperature dependence of the relaxation time was displayed in the inset of figure 3.5, and it was found to be obeyed the Arrhenius law,

$$\tau = \tau_0 \exp(E_a / k_B T), \tag{3.3}$$

where τ_0 is the pre-exponential factor, E_a is the activation energy required for relaxation process. The rapid decrease in τ with increasing temperature was suggestive of an increasing dipole density and a faster polarization process (Wu J et al., 2002). The value of E_a calculated by using equation (3.3) together with the

temperature dependence of τ was found to be about 0.313 eV for the $Li_{0.05}Ti_{0.02}Ni_{0.93}O$ ceramic. Lin et al. (2006) also found that the values of E_a and E_g of each LTNO ceramic were nearly the same in value, as summarized in Table 3.1. These results suggested to the close relationship between the polarization relaxation and the electrical transport properties inside the grains.

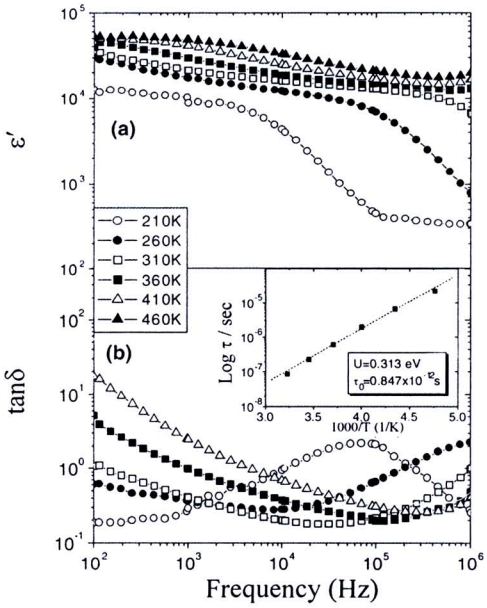

Figure 3.5 Frequency dependence of (a) dielectric constant (ε′) and (b) loss tangent (tanδ) at various temperatures for the $Li_{0.05}Ti_{0.02}Ni_{0.93}O$ ceramic; inset shows the Arrhenius plot for the relaxation time (Adapted from Wu J et al., 2002).

Table 3.1 The values of the dielectric constant (ε′) at 1 kHz and room temperature and the activation energies of the $Li_xTi_yNi_{1-x-y}O$ ceramics.

$Li_xTi_yNi_{1-x-y}O$ sample	ε′	Activation energy (eV)	
		Relaxation (E_a)	Grain conduction (E_g)
$Li_{0.10}Ti_{0.02}Ni_{0.88}O$	6.1×10^4	0.221	0.206
$Li_{0.05}Ti_{0.02}Ni_{0.93}O$	1.8×10^4	0.313	0.309
$Li_{0.10}Ti_{0.05}Ni_{0.85}O$	1.3×10^4	0.373	0.377

(Lin et al., 2006a)

In the case of LTNO ceramics system, the close relationship between the dielectric constant and E_g was also observed, as revealed in Table 3.1. E_a and the related E_g were found to be decreased with an increase in the Li doping concentration; in contrast, both values of the LTNO system could be increased by increasing the Ti doping concentration. As previously reported (van Houten, 1960), doping with ~1%Li into NiO, the conduction activation energy decreased from 0.9 to 0.3 eV at temperature below 500 K, and from 0.6 to about 0.2 eV at temperature above 500 K. With increasing the concentration of the Li doping (5%–10%), a further decrease in activation energy was found to be 0.18 eV below 500 K and 0.14 eV above 500 K. Both experimental results were found to be very similar, E_g decreased with increasing the Li doping ions. Because of the similar ionic radii of Ni^{2+} (0.69 Å) and Ti^{4+} (0.68 Å), the Ni^{2+} ions in NiO crystal lattice could be replaced by the Ti^{4+} doping ions (Lin et al., 2005b). In the LTNO ceramics, when the NiO ceramic was doped with Ti^{4+} ions, defects could, therefore, be introduced into the NiO crystal lattice, which were ascribed by the notation of Kröger and Vink, i.e.,

$$TiO_2 \xrightarrow{NiO} Ti_{Ni}^{\bullet\bullet} + V_{Ni}'' + 2O_o^x, \tag{3.4}$$

where $Ti_{Ni}^{\bullet\bullet}$ is the Ti ion sitting on the Ni lattice site with two positive charges and V_{Ni}'' is the Ni vacancy with double negative charge. According to equation (3.4) and the

data in Table 3.1, the increase in E_g (from 0.206 to 0.377 eV) with the increase of the Ti doping ions (from 0.02 to 0.05 mol) might be attributed to the effect of the $Ti_{Ni}^{\bullet\bullet}$ defects (Lin et al., 2006a). Based on the close relationship between the polarization relaxation and electrical transport inside the grains, it likely seems that the decrease in the dielectric constant of the LTNO ceramics might be related to the increase in E_g rather than that of the increase in grain boundary thickness. However, the supported experimental data are still missing.

3.2 Giant dielectric response in other NiO-based ceramic systems

Lin et al. (2004) have reported that the giant dielectric response in the NiO-based ceramics could also be found in a (Li, Al)-doped NiO (abbreviated as LANO) system. The apparent high dielectric constant of the LANO ceramics was ascribed to the Maxwell-Wagner polarization mechanism just like the LTNO system. It was found that the dielectric constant of the LANO ceramics decreased with an increase in the concentration of Al doping, as demonstrated in figure 3.6. This behavior was similar to that observed in the LTNO system (Wu J et al., 2002). Based on the simple series layer model, the increase in the thickness of the grain boundary due to the accumulation of the Al dopant was used to describe the observed decrease in the dielectric constant of the LANO ceramics. However, the analysis of the microstructure and phase composition of the LANO polycrystalline ceramics is still missing.

Moreover, the giant dielectric properties of the NiO-based ceramics were also observed in the (Li, Si)-doped NiO (abbreviated as LSNO) polycrystalline ceramic system (Lin et al., 2005a). The special core/shell structure was exhibited in this ceramic system. The EDS results revealed that the Si dopant was rich at the grain boundaries of the LSNO ceramics, but indigent inside the grains. The second phase of Ni_2SiO_4 was detected from the XRD pattern of the LSNO ceramics; thus, it was suggested that the second phase relates to the Si-rich boundary. As a result, the microstructural model of the LSNO system was created, consisting of the Ni_2SiO_4-shell and the core of semiconducting Li-doped NiO particle. Through the microstructure and phase composition analyses and the impedance spectroscopy, it

was concluded that the Ni_2SiO_4 phase was accumulated at the grain boundaries and acted as the insulating layers enclosing the semiconducting grains of the Li-doped NiO. The effect of the high-valent cations doping on the dielectric constant of the LSNO was found to be similar to those observed in the LTNO (Wu J et al., 2002; Lin et al., 2006a) and LANO (Lin et al., 2004) systems. The giant dielectric constant of the LSNO ceramics decreased with increasing the Si concentration, as clearly seen in figure 3.7. The high dielectric response in the LSNO ceramics was suggested to the Maxwell-Wagner polarization and the thermally activated mechanisms.

The dielectric relaxation behavior of the LSNO ceramics was also studied at different temperatures and frequencies, as demonstrated in figure 3.8 (Lin et al., 2005a). The dielectric spectra of the LSNO ceramics exhibited the steplike decrease and the corresponding peak of the loss tangent, which shifted to higher frequencies with increasing the temperature. The value of E_a of each LSNO ceramic was found to be almost the same as its E_g value. The observed close relationship between the polarization and the electrical transport in the grain interiors of the LSNO ceramics was similar to that observed in the LTNO ceramics (Lin et al., 2006a).

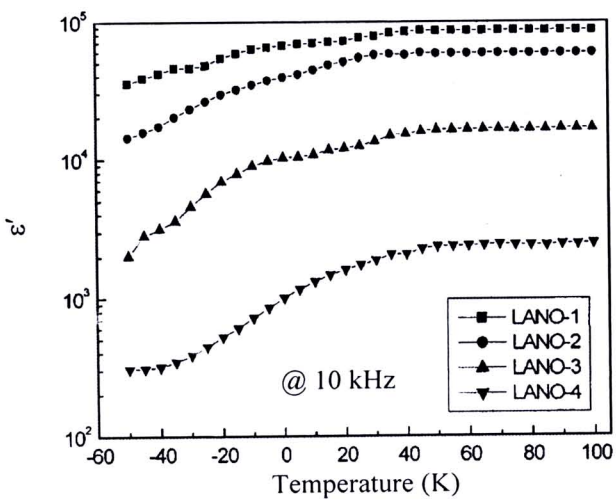

Figure 3.6 Temperature dependence of the dielectric constant (ε′) at the frequency of 10 kHz for the $Li_{0.04}Al_{0.02}Ni_{0.94}O$ (LANO-1), $Li_{0.04}Al_{0.04}Ni_{0.92}O$ (LANO-2), $Li_{0.04}Al_{0.06}Ni_{0.90}O$ (LANO-3), and $Li_{0.04}Al_{0.10}Ni_{0.86}O$ (LANO-4) samples (Adapted from Lin et al., 2004).

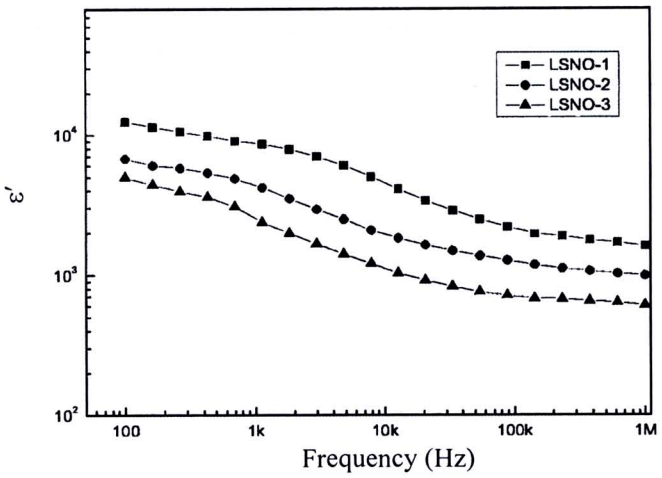

Figure 3.7 Frequency dependence of the dielectric constant (ε′) at the room temperature for the LSNO ceramics with different contents of Si doping, i.e., $Li_{0.01}Al_{0.05}Ni_{0.94}O$ (LSNO-1), $Li_{0.01}Al_{0.15}Ni_{0.84}O$ (LSNO-2), and $Li_{0.01}Al_{0.25}Ni_{0.74}O$ (LSNO-3) (Adapted from Lin et al., 2005a).

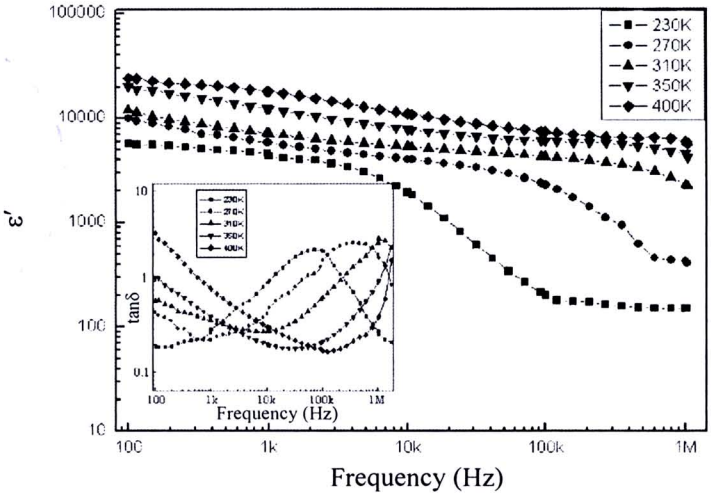

Figure 3.8 Frequency dependence of the dielectric constant (ε′) at several temperatures for the $Li_{0.01}Si_{0.05}Ni_{0.94}O$ ceramic; inset shows the frequency dependence of loss tangent (tanδ) at selected temperatures (Adapted from Lin et al., 2005a).

Considering the core/shell microstructure of the LSNO ceramics, the complex dielectric permittivity of the alternating layer having different dielectric constants (ε'_g and ε'_{gb}) and different conductivities (σ_g and σ_{gb}) are (Raevski et al., 2003);

$$\varepsilon^*_g = \varepsilon'_g - j\sigma_g / \omega, \tag{3.5}$$

$$\varepsilon^*_{gb} = \varepsilon'_{gb} - j\sigma_{gb} / \omega, \tag{3.6}$$

where the subscripts g and gb represent to the grain and grain boundary, respectively. At small conductivities, the total complex dielectric (ε^*) can be quantitatively approximated by:

$$\varepsilon^* = L\left(\frac{t_g}{\varepsilon^*_g} + \frac{t_{gb}}{\varepsilon^*_{gb}}\right)^{-1}, \tag{3.7}$$

where t_g is the particle size of the conducting grain, t_{gb} is the thickness of boundary layer, and $L = t_g + t_{gb}$. Since $L >> t_{gb}$ and $\sigma_g >> \sigma_{gb}$, equation (3.7) can be simplified as

$$\varepsilon^* = \frac{\varepsilon_g}{a} + \left(\frac{\varepsilon_{gb}}{a\delta}\right)\left(\frac{1}{1 + j\omega\tau}\right), \tag{3.8}$$

where $a = 1 + \delta\varepsilon_g / \varepsilon_{gb}$, $\tau = a\varepsilon_{gb} / \delta\sigma_g$, $\delta = t_{gb} / L$.

At zero or very low frequency, the equation (3.8) can be further simplified as,

$$\varepsilon' = \frac{L\varepsilon_{gb}}{t_{gb}}. \tag{3.9}$$

Equation (3.9) indicated that the dielectric constant could be controlled by the thin non-conducting layer or grain boundary. As for the LSNO ceramics, the average Li-doped NiO grain size was found to be about 2.0 μm, and the thickness of grain boundary region with increasing doping SiO_2 was estimated to be about 5–15 nm, and the dielectric constant of Ni_2SiO_4 was about 30 (Lin et al., 2005a). Therefore, the dielectric constant at low frequency will be 4,000–12,000, which were in good agreement with the experimental data.

It was reported that the incorporation of higher–valent cations, e.g., Ta^{5+}, V^{5+}, and W^{6+}, into the Li-doped NiO ceramics can exhibit the giant dielectric properties in these NiO-based systems. For a (Li, Ta)-doped NiO system (abbreviated as LTaNO) (Hsiao et al., 2007), it was found that the concentration of Ta had a remarkable influence on the dielectric properties of the LTaNO ceramics. The phase composition of the LTaNO ceramics characterized by the XRD technique revealed that the XRD patterns of the LTaNO ceramics consisted of the major phase of NiO and the minor phase of $NiTa_2O_6$, as revealed in figure 3.9. No peak shift was observed, indicating a lack of mutual solubility between the two phases. The relative amounts of the NiO and $NiTa_2O_6$ phases could be calculated by measuring the major peak intensities for NiO (200) and $NiTa_2O_6$ (110) phases as

$$NiO(\%) = \frac{I_{NiO}(200)}{I_{NiO}(200) + I_{NiTa_2O_6}(110)} \times 100(\%). \tag{3.10}$$

The calculated results revealed that the amounts of the NiO cubic phase for the compositions of $Li_{0.01}Ta_{0.01}Ni_{0.98}O$, $Li_{0.01}Ta_{0.05}Ni_{0.94}O$, and $Li_{0.01}Ta_{0.10}Ni_{0.89}O$ were found to be 95%, 78% and 61%, respectively. The $NiTa_2O_6$ phase increased with increasing the concentration of Ta doping ions. Although the chemical compositions of the grain and grain boundary of the LTaNO were not investigated, Hsiao et al. (2007) have deduced that the microstructure of the LTaNO ceramics was equivalent to the LTaNO-$NiTa_2O_6$ composites. Therefore, the giant dielectric properties of the LTaNO ceramics might be related to the existing multiphase, which have large amounts of interfaces.

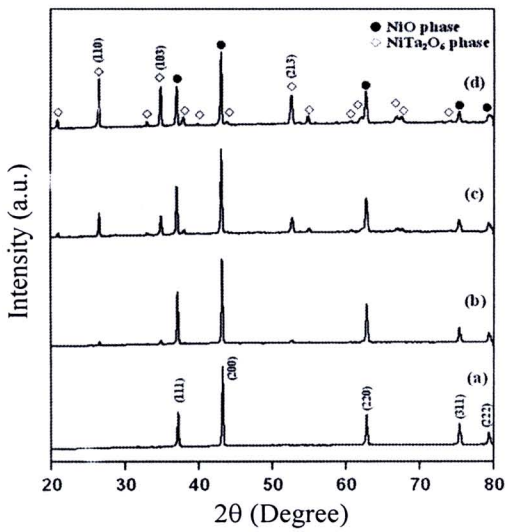

Figure 3.9 XRD patterns of (a) NiO, (b) $Li_{0.01}Ta_{0.01}Ni_{0.98}O$, (c) $Li_{0.01}Ta_{0.05}Ni_{0.94}O$, and (d) $Li_{0.01}Ta_{0.10}Ni_{0.89}O$ ceramics (Adapted from Hsiao et al., 2007).

Due to a small difference in ionic radius of the doping ions of Li^+ and Ta^{5+}, and the host Ni^{2+} ion, Ni^{2+} sites in NiO crystal lattice can occupied by the Ta^{5+} and Li^+ doping ions. Thus, defects could be introduced into the NiO crystal lattice. This could be expressed as (Hsiao et al., 2007),

$$Ta_2O_5 \xrightarrow{NiO} 2Ta_{Ni}^{\bullet\bullet\bullet} + 3V_{Ni}'' + 5O_o^x, \tag{3.11}$$

$$Li_2O \xrightarrow{NiO} 2Li_{Ni}' + V_O^{\bullet\bullet} + O_o^x, \tag{3.12}$$

where $Ta_{Ni}^{\bullet\bullet\bullet}$ is the Ta ion sitting on the Ni lattice site with three positive charges, Li_{Ni}' is the Li ion sitting on the Ni lattice with a single negative charge, and $V_O^{\bullet\bullet}$ is the oxygen vacancy with double positive charges. The combination of $V_O^{\bullet\bullet} - 2Li_{Ni}'$, and $2Ta_{Ni}^{\bullet\bullet\bullet} - 3V_{Ni}''$ might be formed due the coulombic attraction (Hsiao et al., 2007). Therefore, it was proposed that the $2Li_{Ni}' - V_O^{\bullet\bullet}$ and $2Ta_{Ni}^{\bullet\bullet\bullet} - 3V_{Ni}''$ complex defects also had a contribution to the total dielectric response in the LTaNO ceramics. Consequently, the observed high dielectric constant of the LTaNO ceramics was

attributed to both of the space charge and orientational (dipolar) polarizations. It is important to note that the dielectric properties of the LTaNO ceramics seem to be different from that observed in the original high-permittivity LTNO ceramics. As demonstrated in figure 3.10, the dielectric constant of the 5%Ta-doped Ni(Li)O ceramic is larger than those of the 1%Ta- and 10%Ta-doped Ni(Li)O ceramics. The physical explanation of this observation is still missing and unclear.

For (Li, V)- and (Li, W)-doped NiO systems (abbreviated as LVNO and LWNO, respectively) (Chen GJ et al., 2009), the dielectric constants of these two ceramics were found to be large, $\varepsilon' \sim 2\times10^3$ and $\sim 2\times10^4$ for the $Li_{0.01}V_{0.05}Ni_{0.94}O$ and $Li_{0.01}W_{0.05}Ni_{0.94}O$ ceramics, respectively. The dielectric spectrum of the LVNO ceramic exhibited two steplike decreases at high and low frequency ranges, corresponding to two respective peaks in loss tangent, as illustrated in figure 3.11. This result indicated that there exist two sets of dielectric relaxations in the LVNO ceramic. The dielectric spectrum of the LWNO ceramic was found to be three dielectric relaxations, but only the medium-frequency relaxation was dominated and clearly observed. Unfortunately, the careful investigation and explanation of these relaxations is still ambiguous

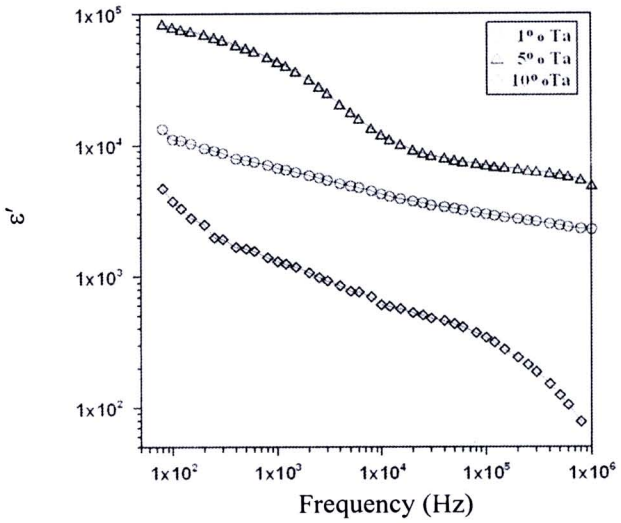

Figure 3.10 Frequency dependence of the dielectric constant (ε′) of the LTaNO ceramics with different Ta doping concentrations (Adapted from Hsiao et al., 2007).

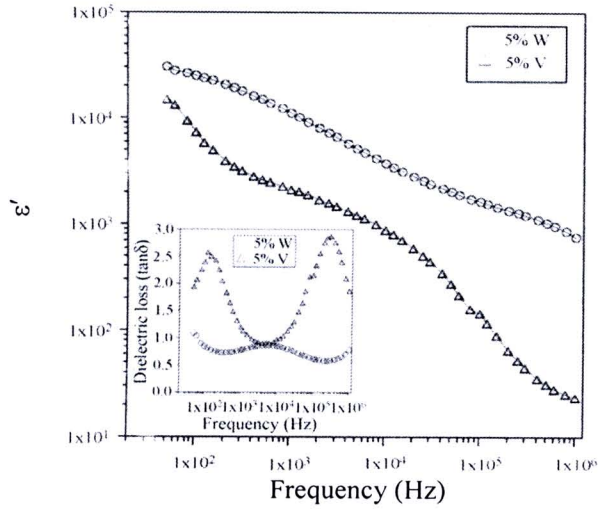

Figure 3.11 Frequency dependence of the dielectric constant (ε′) of the $Li_{0.01}V_{0.05}Ni_{0.94}O$ and $Li_{0.01}W_{0.05}Ni_{0.94}O$ ceramics; inset shows the frequency dependence of the loss tangent (tanδ) (Adapted from Chen GJ et al., 2009).

3.3 Dielectric abnormities in Zr-doped NiO ceramics

As previous reports, it was demonstrated that the giant dielectric response in the NiO-based ceramics could be exhibited by co-doping with the monovalent cation of Li^+ and the higher-valent cations (Wu J et al., 2002; Lin et al., 2004; Lin et al., 2005a; Hsiao et al., 2007). The monovalent cation of Li^+ was used to create the semiconducting grains of the NiO-based ceramics; on the other hand, the higher-valent cations were usually used to form the insulating grain boundaries enclosing the semiconducting grains. This is a basic concept to ascribe the origin of the giant dielectric response in the NiO-based materials. Surprisingly, the giant dielectric properties of the NiO-based ceramics were observed in the Zr-doped NiO (abbreviated as ZNO) polycrystalline ceramics (Chen K et al., 2007), which is a single doped NiO-based ceramic. The frequency dependence of the giant dielectric constant of the ZNO ceramics was demonstrated in figure 3.12, showing the steplike decrease of the dielectric constant at high frequencies. The step-like decrease shifted to higher frequency with increasing temperature, suggesting to the thermally activated mechanism just like the dielectric relaxation behavior of the LTNO and other NiO-

based ceramics. As previous reviews, the polarization relaxation in the LTNO and LSNO ceramics was found to be closely related to the conductivity inside the grain (Lin et al., 2005a; Lin et al., 2006a). As a result, the ceramic with smaller E_g must exhibit a higher dielectric constant (Cheng et al., 2008). However, this relationship could not be used to ascribe the dielectric behavior of the single doped ZNO ceramics, as evidently seen in table 3.2. K Chen et al. (2007) have suggested that the observed high dielectric response in these two ceramics was associated with the grain boundary (internal) layer capacitor effects. The difference in the dielectric constant observed in the $Zr_{0.1}Ni_{0.8}O$ and $Zr_{0.2}Ni_{0.6}O$ ceramics was therefore attributed to the difference in the grain size between them, as summarized in Table 3.2. Note that, the slight different values of E_g and E_{gb} could be suggested that the chemical composition of the grain boundary was slightly different from that of the grain (Sarkar et al., 2008). However, the careful analysis of the microstructure and phase composition of the ZNO ceramics is still missing. Therefore, the evident origin of the high dielectric response in the ZNO is still incomplete.

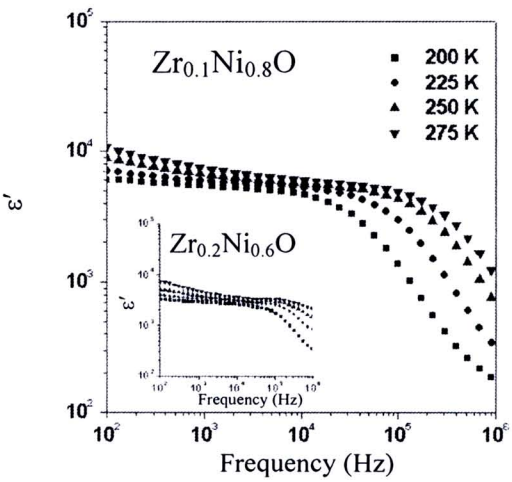

Figure 3.12 Frequency dependence of the dielectric constant (ε′) at selected temperature for the $Zr_{0.1}Ni_{0.8}O$ ceramic; inset shows the frequency dependence of dielectric constant of the $Zr_{0.2}Ni_{0.6}O$ ceramic (Adapted from Chen K et al., 2007).

Table 3.2 The values of the dielectric constant (ε′) at 10 kHz and room temperature, the grain size, and the activation energies of the ZNO ceramics.

sample	ε′	Grain size (μm)	Conduction activation energy (eV)	
			Grain (E_g)	Grain boundary (E_{gb})
$Zr_{0.1}Ni_{0.8}O$	~8 000	~20	0.155	0.195
$Zr_{0.2}Ni_{0.6}O$	~3 000	~15	0.135	0.157

(Chen K et al., 2007)

3.4 Effect of various valence states of the *A*-dopants on dielectric and electrical properties of the $A_{0.03}Ti_{0.10}Ni_{0.87}O$, where A=K^+, Mg^{2+}, Y^{3+}

As previous reports (Lin et al., 2005a; Lin et al., 2006a), the close relationship between the polarization relaxation of the NiO-based ceramics and their electrical transport inside the grains was observed. Therefore, the electrical properties of the grains would ultimately decide the dielectric properties of these ceramics. The variation of the electrical properties inside the grains of the NiO-based ceramics may be induced by doping different valence states of the dopants into NiO. Cheng et al. (2008) indicated that the various valence states of *A*-doping, i.e., K^+, Mg^{2+}, and Y^{3+}, had remarkable influence on the dielectric properties of the $A_{0.03}Ti_{0.10}Ni_{0.87}O$ ceramics. It was revealed that the large variation of the conduction activation energies in the grain interiors could affect to the dielectric properties of the $A_{0.03}Ti_{0.10}Ni_{0.87}O$ ceramics. The values of the dielectric constant and E_g of the $K_{0.03}Ti_{0.10}Ni_{0.87}O$ (KTNO), $Mg_{0.03}Ti_{0.10}Ni_{0.87}O$ (MTNO), and $Y_{0.03}Ti_{0.10}Ni_{0.87}O$ (YTNO) ceramics were summarized in Table 3.3. The KNTO ceramic with smaller E_g exhibited a higher dielectric constant among these three ceramics. Cheng et al. (2008) have proposed that this result might be due to that the polarization process was closely related to the conduction of the charge carriers inside the grains (Lin et al., 2006a). Therefore, the discrepancy in the activation energies caused by K^+, Mg^{2+}, and Y^{3+} doping resulted to the observed various dielectric response in these three ceramics. Looking carefully at Table 3.3, however, the dielectric constant of the MTNO ceramic was found to be larger that that of the YTNO ceramic, while the value of E_g of the MTNO ceramic

was found to be larger. This implies that the dielectric properties of the NiO-based ceramics might be contributed by the other factors such as the grain size, the feature of microstructure, and etc. However, the experimental results supported these assumptions are rare. As illustrated in figure 3.13, the dielectric spectra of the YTNO ceramic exhibited the steplike decrease of the dielectric constant at low temperature, which was similar to those observed in the other NiO-based ceramics. Above the temperature of this step, the dielectric constants were found to be nearly independent of temperature for the frequency of 10^2 Hz. This dielectric behavior could be ascribed to the migration of excited electrical particles at high temperatures, which has also been observed in $CaCu_3Ti_4O_{12}$ (Li, Schwartz, 2007), $Ca(Fe_{1/2}Nb_{1/2})O_3$, and $Sr(Fe_{1/2}Nb_{1/2})O_3$ systems (Liu YY et al., 2007a,b).

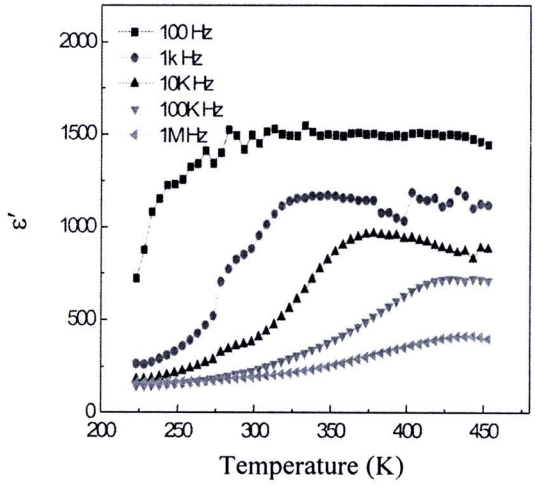

Figure 3.13 Temperature dependence of the dielectric constant (ε′) of the $Y_{0.03}Ti_{0.10}Ni_{0.87}O$ ceramic at selected frequencies (Adapted from Cheng et al., 2008).

Table 3.3 The values of the dielectric constant (ε′) at 1 kHz and room temperature and the activation energies of the $A_{0.03}Ti_{0.10}Ni_{0.87}O$ ceramics.

sample	ε′	Conduction activation energy (eV)	
		Grain (E_g)	Grain boundary (E_{gb})
KTNO	10 680	0.242	0.451
MTNO	3 920	0.424	0.565
YTNO	850	0.372	0.554

(Cheng et al., 2008)

3.5 Effect of various types of monovalent cations on the microstructure and dielectric properties of $A_{0.05}Ti_{0.02}Ni_{0.93}O$ ceramics, where A=Li^+, Na^+, K^+

Because of a small difference in the ionic radius of Li^+ (0.60 Å) and Ni^{2+} (0.69 Å) ions (Lin et al., 2005b), the Li^+ doping ions can replace the Ni^{2+} sites in NiO crystal lattice. As a result, the conductivity of the bulk NiO can be enhanced by doing with such monovalent Li^+ ions due to the introduction of Ni^{3+}. Thus, it is possible that the conductivity of the bulk NiO may be improved by doping with the other monovalent cations such as Na^+ and K^+, if such ions can substitute the Ni sites in NiO crystal lattice. It was found that the (Na, Ti)- and (K, Ti)-doped NiO (abbreviated as NaTNO and KTNO, respectively) polycrystalline ceramics could also be exhibited the high dielectric properties (Jana et al., 2006; Jana et al., 2007a,b,c,d; Jana et al., 2008). The experimental results revealed that the Na^+ and K^+ doping had great effects on both of the microstructure and dielectric properties of the NiO-based ceramics. As revealed in figures 3.14(a) to 3.14(c), the morphologies of the NiO-based ceramics were significantly different for the NaTNO ceramic compared with those of the other two systems. The NaTNO ceramic showed a special step-pyramidal or hillocks morphology with looser grain boundaries than for LTNO and KTNO ceramics.

The different microstructures of ceramics are usually attributed to the difference in the diffusivity of ions in the ceramics, which is related linearly to their electrical conductivity. In this case, it was proposed that the large difference in the electrical conductivity of Na with respect to the parent Ni atom might be related to this special type of morphology appearing in the NaTNO system (Jana et al., 2008).

Moreover, it was also found that the microstructure of the NaTNO system exhibited the large portion of porosity compared with the LTNO and KTNO systems. Either of the large divergence of the ionic radius mismatch of substitute atom with the parent and the Pilling–Bedworth ratio (PBR) might relate to this observation (Jana et al., 2008). The difference in ionic radius of various monovalent ions from that of Ni^{2+} are 0.12, 0.23 and 0.55 Å, respectively, for Li^{+}, Na^{+} and K^{+}. In spite of the largest mismatch in ionic radii of Ni^{2+} with K^{+} compared with that of Li^{+} or Na^{+}, the NaTNO ceramic showed the largest pores and the KTNO ceramic possessed the smallest pores. Therefore, the observed anomaly in surface morphologies of these three ceramics could not be explained by the divergence in ionic radii. According to the PBR, it is well known that tensile stress or compressional stress is produced at the oxide layer if the PBR is less than unity or greater than unity, respectively. Intensity of this stress increases when the PBR of a metal differs from unity. The difference in the PBR from unity for Na was found to be ~0.42 (but for K ~0.59 and Li ~0.43) (German, Munir, 1974). This value was much less than the difference (~0.60) for Ni. Therefore, compressional stress or tensile stress can not compensate each other locally in Na and Li doped ceramics, and thus more pores (or crack) were observed in these ceramics. The difference in the PBR from unity being the lowest (~0.42) for Na, the NaTNO system showed relatively a large number of pores.

For the dielectric properties, it was also found that the different microstructures of these three ceramics led to the variation of the dielectric properties of the ceramics. The low-frequency dielectric constant of the NaTNO ceramic exhibited the lowest value among three ceramics, as shown in figure 3.14(d). Generally, the low-frequency dielectric response is attributed to the space charge polarization at the interface layers such as grain boundary and/or sample–electrodes (Hence, West, 1990). According to the SEM images, the low-frequency dielectric properties of the NaTNO should be associated with the grain boundary effect rather than that of the electrode effect due to the looser grain boundary.

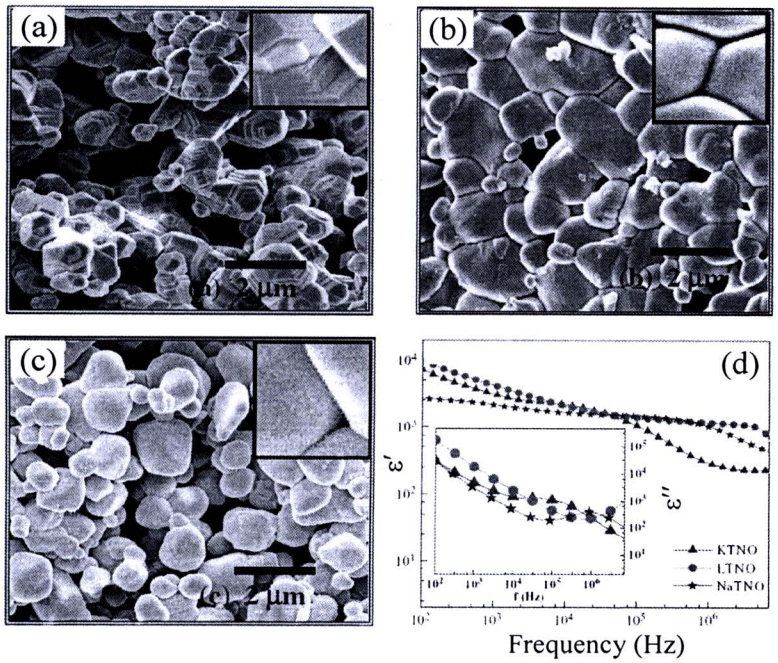

Figure 3.14 (a)-(c) SEM images of the surface morphologies of the NaTNO, KTNO, and LTNO ceramics, respectively. (d) Frequency dependence of the dielectric constant (ε′) at room temperature for the NiO-based ceramics doping with various monovalents (Adapted from Jana et al., 2008).

3.6 High dielectric constant and low dielectric loss in (K, Ti)-doped NiO ceramics

Since the discovery of the giant dielectric constant in the (Li, Ti)-doped NiO ceramics, it had been believed that this material was a promising dielectric material for future applications. However, the values of the dielectric loss of all high-permittivity NiO-based ceramics are still too large, which is a major obstacle for practical applications. Jana et al. (2006) have reported the giant dielectric constant (~10^4-10^5) with vary low loss (~0.03 at room temperature and frequency of 100 Hz) in the $K_{0.05}Ti_{0.02}Ni_{0.93}O$ ceramic, which was synthesized by a solid state reaction method. As shown in figure 3.15, the temperature dependence of the dielectric constant and loss tangent of the $K_{0.05}Ti_{0.02}Ni_{0.93}O$ ceramic, two plateaus were appeared in the dielectric spectra of the $K_{0.05}Ti_{0.02}Ni_{0.93}O$ ceramic at temperatures above 300 K and

below 250 K. The giant dielectric constant of this ceramic was observed at temperatures above 300 K and at frequencies below 1 kHz. The values of the loss tangent that lower than 0.05 were observed at frequencies below 1 kHz and temperature range of 250–350 K. As results, it seems that this ceramic shows a high performance for future applications. However, a careful inspection reveals that the giant dielectric constant drop rapidly to the low value when the frequency is higher than 1 kHz corresponding to the increase in the loss tangent due to the relaxation process. This may limit the high frequency applications for this material.

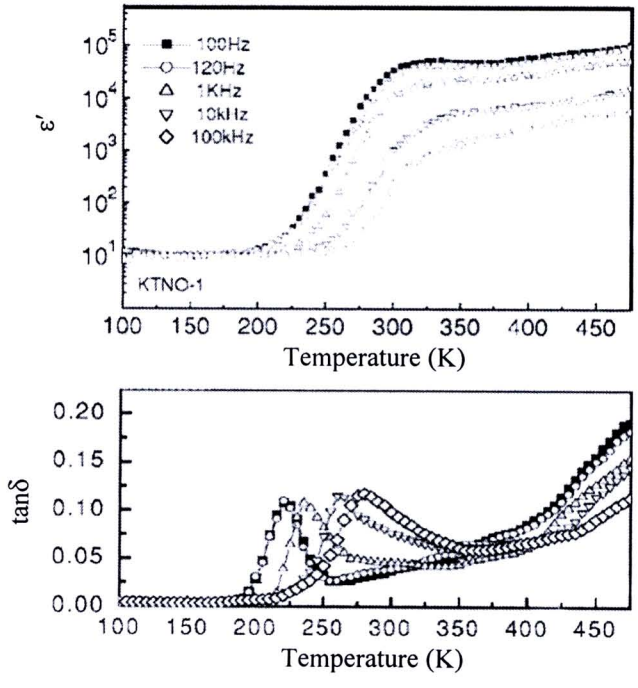

Figure 3.15 Temperature dependence of (a) the dielectric constant (ε′) and (b) the loss tangent (tanδ) of the $K_{0.05}Ti_{0.02}Ni_{0.93}O$ ceramic at different frequencies (Adapted from Jana et al., 2006).

To understand the dielectric relaxation behavior of the $K_{0.05}Ti_{0.02}Ni_{0.93}O$ ceramic, the frequency dependence of the dielectric properties of the $K_{0.05}Ti_{0.02}Ni_{0.93}O$ ceramic was studied at various temperatures. As shown in figure 3.16 (Jana et al., 2006), two dielectric relaxations were observed in the dielectric spectra of the $K_{0.05}Ti_{0.02}Ni_{0.93}O$ ceramic; high– and medium–frequency relaxations. However, only high–frequency relaxation was analyzed, as illustrated in the inset. The analysis of the dielectric relaxation revealed that the estimated relaxation activation energy was found to be about 0.362 eV. The values of the dielectric constant, loss tangent, and calculated activation energies of (K, Ti)-doped NiO ceramics with different contents of K doping were summarized in table 3.4. It is clearly seen from the table that the dielectric constant of these ceramics increases with increasing the K concentration. The values of E_a and dc conduction activation energy were found to be nearly the same in value for the $K_{0.05}Ti_{0.02}Ni_{0.93}O$ ceramic. The close relationship between the dielectric (polarization) and electrical properties was similar to that observed in the LTNO ceramics (Lin et al., 2006a). However, the difference in dielectric behavior between these two ceramic systems could be observed, the dc conduction activation energy did not change with the concentration of K doping.

Table 3.4 The values of the dielectric constant (ε′) and loss tangent tanδ at 100 Hz and 300 K and the activation energies of the (K, Ti)-doped NiO ceramics.

sample	ε′	tanδ	Activation energy (eV)	
			Relaxation (E_a)	dc conduction
$K_{0.05}Ti_{0.02}Ni_{0.93}O$	33 991	0.03	0.362	0.364
$K_{0.25}Ti_{0.02}Ni_{0.73}O$	159 409	9.61	-	0.358
$K_{0.30}Ti_{0.02}Ni_{0.68}O$	214 791	25.41	-	0.350

(Jana et al., 2006)

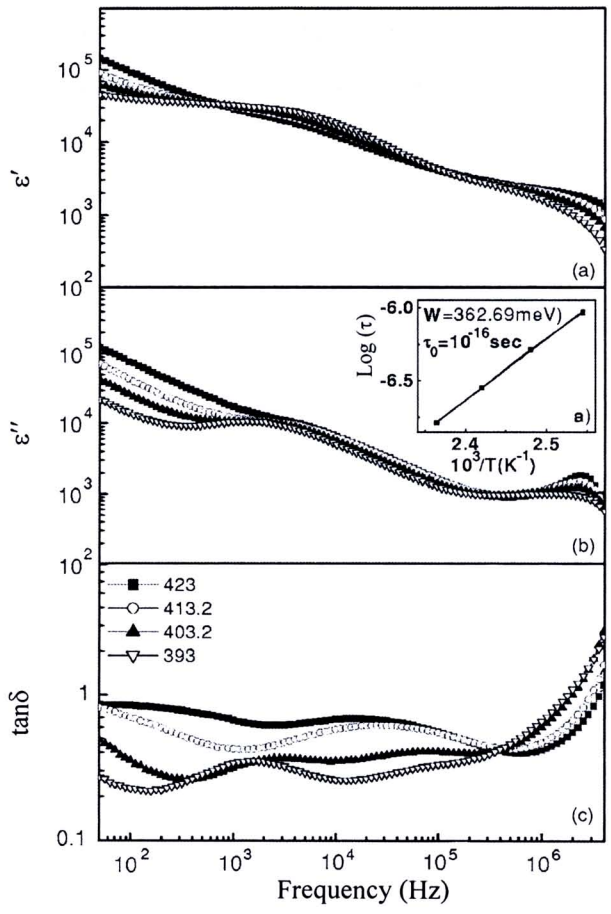

Figure 3.16 Frequency dependence of the dielectric properties of the $K_{0.05}Ti_{0.02}Ni_{0.93}O$ ceramic at various temperatures: the real (ε′) and imaginary (ε″) parts of the complex permittivity (ε*=ε′-*j*ε″) and the loss tangent (tanδ=ε″/ε′). The inset shows the Arrhenius plot of the relaxation process (Adapted from Jana et al., 2006).

Jana et al. (2007c) have suggested that the observed giant dielectric response in the KTNO ceramics was attributed to the IBLC effect, which was ascribed based on the Maxwell-Wagner polarization. The dielectric constant of the KTNO ceramics was found to be decreased with an increase in the concentration of Ti (Jana et al., 2007c). This result was attributed to the increase in the thickness of the grain boundary. However, the evident distribution of Ti doping in the microstructure of the KTNO ceramics was never reported. Although the dielectric behavior of the KTNO ceramics was similar to that observed in the LTNO ceramics, the important question

remains unclear. Because of the large difference in ionic radius between Ni^{2+} (0.69 Å) and K^{+} (1.24 Å) (Lin et al., 2005b; Jana et al., 2008), thus, Can the K^{+} doping ions replace the Ni^{2+} sites in the NiO crystal lattice? Moreover, the dielectric relaxation of the $K_{0.05}Ti_{0.02}Ni_{0.93}O$ ceramic was found in the temperature range of 250–300 K, as clearly seen in figure 3.15, but their relaxation behavior was characterized in the temperature range of 393–423 K, as revealed in figure 3.16. Therefore, it is unsuitable to suggest that the polarization relaxation in the KTNO ceramics has a strong relation to the conductivity inside the grains. From these points of view, it seems that the origin of the observed giant dielectric properties of the NiO-based systems is still unclear.

3.7 Defects in (Li, Ti)-doped NiO ceramics system with giant dielectric constant

As discussed in previous section, the giant dielectric constant observed in the NiO-based ceramics was suggested to be attributed to the Maxwell-Wagner polarization at the insulating grain boundary (Wu J et al., 2002; Lin et al., 2004, 2005a, 2006; Maensiri et al., 2007). Up to now, it is widely believed that giant dielectric response in the NiO-based ceramics is associated with the IBLC effect based on the Maxwell-Wagner polarization at the grain boundaries (Manna, De, in press; Dekhel, 2009). Besides the grain boundary effect, however, some researches have suggested that the giant dielectric constant of the NiO-based ceramics might also be due to the polarization induced by defects, e.g., $[2Li'_{Ni}V_O^{\bullet\bullet}]$, $[Ti_{Ni}^{\bullet\bullet}V''_{Ni}]$, and $[2Ta_{Ni}^{\bullet\bullet\bullet}3V''_{Ni}]$ (Lin et al., 2005b; Hsiao et al., 2007). Therefore, it was proposed that the giant dielectric constant response of the NiO-based ceramics was enhanced partially by the IBLC mechanism, and partially by the polarization of defect dipoles (Lin et al., 2005b).

Most recently, P Wu et al. (2009) have combined first-principles, statistical, and phenomenological methods to investigate the electronic and dielectric properties of the NiO-based material, and to clarify the nature of the observed giant dielectric response. They have suggested that the giant dielectric response in the NiO-based ceramics may be associated with the small polaron hopping inside semiconducting

grains. The theoretical results revealed that the small polaron hoping on dopant levels was the dominant mechanism for the giant dielectric response in the NiO-based ceramics. Thus, they have argued that the giant dielectric response in the NiO-based ceramics was not related to the microstructure of the ceramics, e.g., grain size and morphologies. Unfortunately, the experimental data supported the small polaron hopping model is still missing.